Journal of Theoretical Biology 286 (2011) 31–40

Contents lists available at ScienceDirect

Journal of Theoretical Biology

journal homepage: www.elsevier.com/locate/yjtbi

High-frequency electric field and radiation characteristics of cellular microtubule network

D. Havelka [a,*], M. Cifra [b], O. Kučera [b,c], J. Pokorný [b], J. Vrba [a]

[a] Department of Electromagnetic Field, Faculty of Electrical Engineering, Czech Technical University in Prague, Czech Republic
[b] Institute of Photonics and Electronics, Academy of Sciences of the Czech Republic, Czech Republic
[c] Department of Circuit Theory, Faculty of Electrical Engineering, Czech Technical University in Prague, Czech Republic

ARTICLE INFO

Article history:
Received 20 February 2011
Received in revised form
10 July 2011
Accepted 11 July 2011
Available online 20 July 2011

Keywords:
Bioelectrodynamics
Microtubule network
Cellular power

ABSTRACT

Microtubules are important structures in the cytoskeleton, which organizes the cell. Since microtubules are electrically polar, certain microtubule normal vibration modes efficiently generate oscillating electric field. This oscillating field may be important for the intracellular organization and intercellular interaction. There are experiments which indicate electrodynamic activity of variety of cells in the frequency region from kHz to GHz, expecting the microtubules to be the source of this activity. In this paper, results from the calculation of intensity of electric field and of radiated electromagnetic power from the whole cellular microtubule network are presented. The subunits of microtubule (tubulin heterodimers) are approximated by elementary electric dipoles. Mechanical oscillation of microtubule is represented by the spatial function which modulates the dipole moment of subunits. The field around oscillating microtubules is calculated as a vector superposition of contributions from all modulated elementary electric dipoles which comprise the cellular microtubule network. The electromagnetic radiation and field characteristics of the whole cellular microtubule network have not been theoretically analyzed before. For the perspective experimental studies, the results indicate that macroscopic detection system (antenna) is not suitable for measurement of cellular electrodynamic activity in the radiofrequency region since the radiation rate from single cells is very low (lower than 10^{-20} W). Low noise nanoscopic detection methods with high spatial resolution which enable measurement in the cell vicinity are desirable in order to measure cellular electrodynamic activity reliably.

© 2011 Elsevier Ltd. All rights reserved.

1. Introduction

Electrodynamic activity of eukaryotic cells is a topic, which is gaining considerable theoretical and experimental support in recent years. In the 1960s Fröhlich postulated and theoretically treated a concept in which he presented the possible existence of the mechanical vibrations of electrically polar structures in living cell causing generation of electric oscillations around and in the cell. Firstly, he proposed electrically polar longitudinal vibrations interacting with an elastic field, giving rise to coherent cellular electric oscillations (Fröhlich, 1968b, 1969). Secondly, he showed that the energy condenses to the lowest frequency mode in his nonlinear model system (Fröhlich, 1968a). Lastly, he estimated that oscillating polar structures are situated in the cellular membrane and their oscillating frequency is in range $10^{11}-10^{12}$ Hz. However, with the advent of deeper understanding of the cellular structure the microtubules emerge as hot candidates for generation of endogenous electrodynamic activity of living cells (Pokorný et al., 1997, 1998).

A possible biological role of the endogenous cellular high-frequency electric field has been analyzed by several authors. Its role has been proposed in long-range protein interactions (Fröhlich, 1972, 1975), in chemical reaction transfer and consequently chemical reaction kinetics (Pokorný and Wu, 1998; Pokorný et al., 2005a, 2005b; Pokorný, 2001), in disrupted cellular organization state such as cancer (Fröhlich, 1978; Pokorný et al., 2008), and in intercellular interactions (Pokorný et al., 1983; Pokorný and Fiala, 1994; Pokorný, 2006; Pohl, 1981, 1980; Rowlands et al., 1981, 1982).

The electrodynamics of cellular structures is inseparably connected to the vibrational dynamics of biomacromolecules. Many marvelous biological functions in proteins and DNA and their profound dynamic mechanisms, such as switch between active and inactive states (Chou, 1984b; Chou et al., 2001; Wang and Chou, 2009), cooperative effects (Chou, 1989), allosteric transition (Chou, 1984a, 1987; Schnell and Chou, 2008), intercalation of drugs into DNA (Chou and Mao, 1988), and assembly of microtubules (Chou et al., 1994), can be revealed by studying their internal motions (Chou, 1988) or terahertz frequency motions. Such inferences have been later observed by NMR (Chou et al., 2001), and applied in medical treatments (Gordon, 2007, 2008;

* Corresponding author.
E-mail address: haveldan@fel.cvut.cz (D. Havelka).

0022-5193/$ - see front matter © 2011 Elsevier Ltd. All rights reserved.
doi:10.1016/j.jtbi.2011.07.007

Madkan et al., 2009). Recently, investigation into the internal motion in biomacromolecules and its biological functions is deemed as a 'genuinely new frontier in biological physics' (Vermont Photonics Technologies Corp, 2011). Likewise, to really understand the action mechanism of microtubules, we should consider not only its static structure but also its dynamical character. The electrodynamic behavior of microtubules inevitably underlies electrodynamic activity of living cells.

Electric oscillations of living cells have been experimentally investigated by several authors in the frequency range from kHz (Jelínek et al., 2008, 2009) through MHz (Pohl et al., 1981; Hölzel and Lamprecht, 1994; Hölzel, 2001; Pokorný et al., 2001) to the GHz (Jelínek et al., 2007; Cifra, 2009) region. These pioneering experiments suggest cellular electrodynamic activity in mentioned frequency region, but the measurement systems used were of the threshold sensitivity. It was recently explained (Kučera et al., 2010) which technical prerequisites must be fulfilled by the measurement system which is designed to detect cellular electrodynamic activity in kHz–GHz region. One of the biophysical aspects underlying the technical prerequisites for high gain and low noise of the first pre-amplifier is the obviously low power radiated from the cell. However, there are few theoretical calculations which provide quantitative evaluation of radiated power from cell and electric field intensity around the cell in the high-frequency region. Pokorný carried out calculations where the source of MHz–THz cellular electric oscillations were assumed to be membrane proteins (Pokorný and Wu, 1998; Pokorný, 1990, 1987) (some selected results are also in Pokorný et al., 1983, 1996; Pokorný, 1985). Shein and Kharlanov (2007) and Kharlanov (2006) represented the whole membrane by discrete dipole layer and considered acoustoelectric vibrations of the membrane in MHz–GHz region. The analysis of Russian authors was inspired by the earlier works of Devyatkov, Golant and Betskii (summarized in books Betskii et al., 1988; Devyatkov et al., 1991) who proposed that the acoustoelectric vibrations of the cell membrane can generate electric oscillations in the region of 30–300 GHz and made the first estimation of radiated electromagnetic power from single cell. Results from both groups of authors show clearly that single cell radiation under most conditions is of the power well below 10^{-20} W, thus hardly detectable in far field at room temperature if the exact frequency of radiation is not known a priori. As can be seen, all of these works considered only cell membrane as the source of the oscillatory electric field, although modern findings suggest that cytoskeleton, especially microtubules, is also very probable source of endogenous cellular high-frequency electric oscillations (Cifra et al., 2010d). Work presented here is filling the gap by calculating electric field and radiation of the whole cellular microtubule network.

2. Microtubules

Cytoskeleton is not only the mechanical support of the cell, but also the dynamic structure responsible for dividing the cell in two, for cellular motion and selforganization of the cell. Cytoskeleton is composed of three types of filaments. One of them are microtubules. Microtubules resemble hollow rods with inner and outer diameter 17 and 25 nm, respectively. These structures are mostly composed of 13 protofilaments, see Fig. 1. The subunits of protofilaments are tubulin heterodimers, which are constituted from α- and β-tubulin. Tubulin heterodimer is very polar structure with static dipole moment $p_{AXIS,STATIC} = 337$ D $(1.12 \times 10^{-27}$ C m) (Tuszyński et al., 2005) in the direction of the microtubule axis. In most of eukaryotic cells, microtubule nucleating and organizing center is a centrosome, which is a cell organelle near the nucleus. Microtubules grow up from this center through the cytoplasm to the cell membrane and

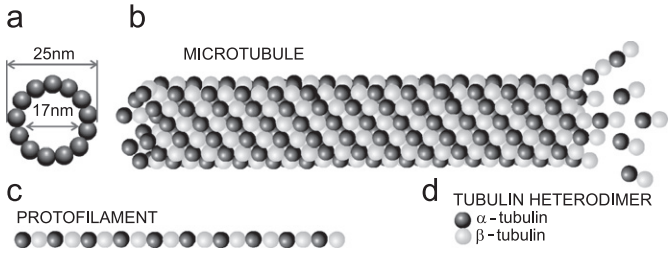


Fig. 1. (a) Cross section of a microtubule. (b) A single microtubule with 13 protofilaments. (c) One protofilament. (d) One tubulin heterodimer.

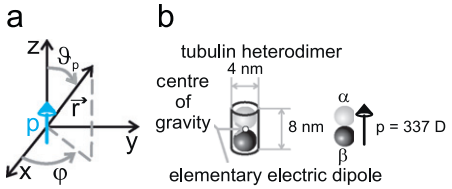


Fig. 2. (a) Dipole moment in the Cartesian coordinate system. (b) Tubulin heterodimer (dimensions and center of gravity).

create intricate network. Together with an extraordinary elasticity, microtubules fulfill all conditions for generation of electric oscillations (Cifra et al., 2010c).

2.1. Electric properties of microtubule

Electric properties of tubulin heterodimer were approximated by an elementary electric dipole (in further text the term "dipole" is used for brevity). Field of such dipole is described by

$$H_\varphi = -\frac{Idl}{4\pi}k^2\sin(\vartheta_p)\left(\frac{1}{jkr}+\frac{1}{(jkr)^2}\right)e^{-jkr} \quad (1)$$

$$E_r = -\frac{Idl}{2\pi}Zk^2\cos(\vartheta_p)\left(\frac{1}{(jkr)^2}+\frac{1}{(jkr)^3}\right)e^{-jkr} \quad (2)$$

$$E_\vartheta = -\frac{Idl}{4\pi}Zk^2\sin(\vartheta_p)\left(\frac{1}{jkr}+\frac{1}{(jkr)^2}+\frac{1}{(jkr)^3}\right)e^{-jkr} \quad (3)$$

where E is the electric field intensity, H is the magnetic field intensity, I is the equivalent current, dl is the length of the dipole, Z is the wave impedance, k is the propagation constant, ω is the angular frequency, p is the dipole moment, j is the imaginary unit ($j^2 = -1$) and other symbols are according to Fig. 2a.

All equations include:

$$Id\vec{l} = j\omega\hat{p} \quad (4)$$

In the near zone the dominant components are with $E \sim 1/(jkr)^3$ and $H \sim 1/(jkr)^2$ and the time-averaged Poynting vector (power density, or Poynting vector in further text, for brevity) composed of these components is zero in lossless medium, because the phase shift between E and H is $\pi/2$. Time-averaged Poynting vector $\vec{S}$ is defined as $\vec{S} = \frac{1}{2}\mathrm{Re}\{\vec{E} \times \vec{H}^*\}$, where Re{} denotes real part of complex number and * denotes complex conjugate.

Every tubulin heterodimer in one microtubule is approximated by elementary electric dipole to obtain the model of electrical properties of microtubule (Fig. 3).

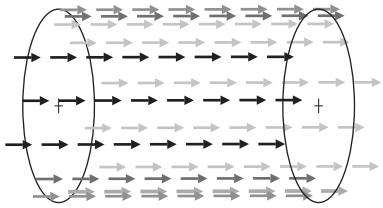


Fig. 3. Model of electrical properties of microtubule. Every arrow represents one dipole.

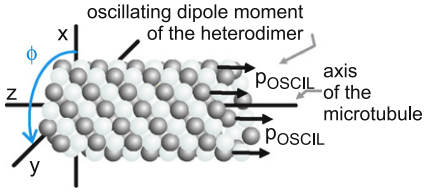


Fig. 4. Location of microtubule in coordinate system and sense of the angles ϑ and ϕ.

3. Method of calculation

Scripts for calculation of electromagnetic field generated by microtubule network were written in Matlab. It had to be dealt with three problems during calculations. The first is the distribution of points on the sphere with the smallest potential energy—to obtain the most symmetric distribution of arbitrary number of microtubules. The second is the rotation of microtubules and then creation of microtubule network. The last problem to deal with was a summation of small and great numerical values. The first problem was analyzed by Bulatov (1996). The solution of problem of microtubule rotation will be described in the following: The microtubule is situated in Cartesian coordinate system (Fig. 4) and coordinates of vector of elementary electric dipoles (both position and direction) are known.[1]

These coordinates were rotated according to the points distributed on the sphere[2] with the smallest potential energy. Two representative models of microtubule network were created in this way. The first model (symmetric) represents the microtubule network of nondividing cell. End points of microtubules' axes are distributed symmetrically and uniformly on the sphere in this model (the axes of microtubules are situated along radius vectors from center of the sphere to end points which are uniformly distributed on the sphere. Uniform distribution was obtained by an algorithm which calculates coordinates of point charges uniformly distributed on sphere—distributed according to their total smallest potential energy) (Fig. 5). This uniform and symmetric distribution of microtubules simulates complete (phase and geometric) symmetry in the cell. The second model (asymmetric) is the model of asymmetric distribution of microtubules (Fig. 6). This model represents microtubule network during mutual cellular interaction or during cellular interaction with solid substrates when cytoskeleton is redistributed. Both models are composed of 100 microtubules, which is reasonable estimate based on electron microscopy studies of eukaryotic cells (Sobel, 1997; Winey et al., 1995; May and Hyams, 1998). Each microtubule in our model is constituted of 1950 heterodimers.[3] We assumed that the ends of microtubules are in direct contact with the cell membrane, i.e. diameter of the model cell is 2.8 μm (0.4 μm diameter of the centrosome $+2\times1.2$ μm of microtubule length).

The problem of summation of small and large numeric values occurred in calculations of power mainly in lossless medium, because the value of field calculated only from near field

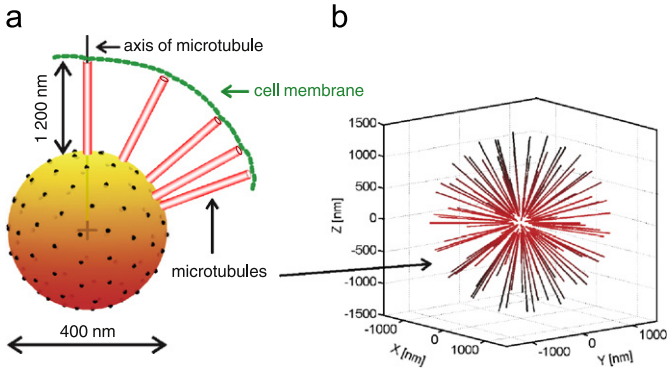


Fig. 5. (a) Model of centrosome with nucleation centers (black points) uniformly and symmetrically distributed on the sphere. (b) The symmetric model of a simple microtubule network with 100 microtubules. The ends of microtubules are distributed according to (a). Each red line represents one microtubule. Centrosome is in no way involved in the generation of mechanical or electric oscillations in the current calculations model, it is depicted here only for clarity and explanation of the geometrical distribution of microtubules. (For interpretation of the references to color in this figure legend, the reader is referred to the web version of this article.)

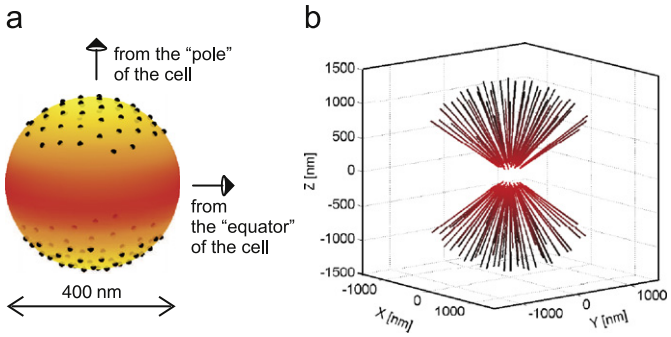


Fig. 6. (a) Model of centrosome with nucleation centers (black points). There are 50 points on each pole. (b) The asymmetric model of a simple microtubule network with 100 microtubules. The ends of microtubules are distributed according to (a). Each red line represents one microtubule. Centrosome is in no way involved in the generation of mechanical or electric oscillations in the current calculations model, it is depicted here only for clarity and explanation of the geometrical distribution of microtubules. (For interpretation of the references to color in this figure legend, the reader is referred to the web version of this article.)

components is much greater than value of field calculated from far field components. This was solved by decomposition of Eqs. (1)–(3) into parts $1/jkr$, $1/(jkr)^2$ and $1/(jkr)^3$ and by calculation of small and large values separately. All three problems and their solutions were described closely by Havelka (2010).

The calculation is executed by vector summation of contributions from all dipoles in the point of space in which the value of electric and/or magnetic field (in further text the term "point" is used for brevity) has to be calculated and then this procedure is repeated for all points in the chosen set (sets included either plane, coaxial surface of microtubule or spherical surface around

[1] Coordinates of the initial point of dipole vector are in the center of gravity of tubulin heterodimer and coordinates of the endpoint of dipole vector depend on angle ϑ. ϑ is the angle between the axis of dipole vector and the axis of microtubule. Thus, $\vartheta=0$ corresponds to case when the dipole vector is parallel with the microtubule axis. In other words, when we consider longitudinal axial oscillations of microtubule (and heterodimer from which it consists), only component of the dipole vector which oscillates significantly is the one which is parallel with the microtubule axis.

[2] Sphere with radius 200 nm represents simple approximation of spherical surface of centrosome, from where the microtubules grow.

[3] Thirteen protofilaments $\times150$ heterodimers in one protofilament, corresponds to the length of 1.2 μm of a single microtubule.

cell). This method was used for calculation of the power radiated from models and electric intensity in radiant distance from a cell membrane. The effect of the cell membrane is neglected in our calculations. To obtain the radiated power P, numerical integration of Poynting vector (power density) was performed over the sphere concentric to cell center using summation $P = \sum_i^N S_i \cdot A_i$ (N, number of elementary surfaces, A_i, i-th surface with S_i power density flowing through it) which is discrete equivalent of continuous integration $P = \int \vec{S}\, d\vec{A}$, where P is the power flowing through the surface A and S is the Poynting vector (power density). Electric field of the whole microtubule network was calculated along the radius vector, either in the direction from the "pole" or from the "equator" (Fig. 6).

4. Parameters used for calculations

Calculations were performed in frequency regions in which various workers have been attempting to measure electric oscillations of cells (Jelínek et al., 2007, 2008, 2009; Pelling et al., 2005; Pohl et al., 1981; Hölzel and Lamprecht, 1994; Hölzel, 2001; Pokorný et al., 2001; Cifra, 2009). Two different surrounding media were taken into account: lossy and lossless. The parameters of surrounding media are in Table 1 (ε_r and σ have subscript 1 for lossy medium and subscript 2 for lossless medium). Longitudinal shift between neighboring protofilaments is 4.92 nm (corresponds to the microtubule lattice A, Tuszyński et al., 2005) as can be seen in Fig. 4. Longitudinal oscillations of tubulin heterodimers are represented by oscillating dipole moment in the direction of microtubule axis ($p_{AXIS,STATIC} = 337$ D static part of dipole moment). We note for clarity that every tubulin in microtubule is oscillating. This follows from the fact that oscillations of microtubules as wholes are considered in this paper. Amplitude of oscillatory component of the tubulin dipole moment around kHz was estimated based on Pelling et al. (2004, 2005). In this work Pelling measured oscillations of yeast cell wall, likely connected with cytoskeleton oscillations, in the amplitude range 1–10 nm, so the amplitude of 1 nm was accepted. Amplitudes of oscillations for higher frequencies are assumed to be of the level of thermal motion amplitude of proteins (Chou, 1988), which is around 0.1 nm. Thus, taking ratio of the oscillatory amplitude (1 and 0.1 nm) and the length of the dipole (tubulin heterodimer length of 8 nm) amplitude of the dipole oscillatory component were estimated: for kHz $p_{OSCIL1} = \frac{1}{8} p_{AXIS,STATIC}$ and for higher frequencies $p_{OSCIL2} = \frac{0.1}{8} p_{AXIS,STATIC}$.

Oscillations of tubulin heterodimers in one protofilament were approximated by longitudinal oscillations of the chain of rigid particles of two types, optical branch (Kittel, 1976). Optical branch is able to generate and absorb electromagnetic field effectively. Movement of particles (tubulin heterodimers) and corresponding oscillations of the dipole moment are described by spatial modulation function:

$$p_m = p_{OSCIL} \cdot \sin(mv) \tag{5}$$

Table 1
Parameters of surrounding medium around microtubules and cell model for eight frequencies. ε_r and σ have subscript 1 for lossy medium and subscript 2 for lossless medium.

f (Hz)	1 k, 1 M, 10 M, and 100 M	1 G	10 G	42 G	100 G
ε_{r1} (–) (relative permittivity)	81	81	71	20	10
σ_1 (S/m) (conductivity)	1	1.33	17.22	39.67	68.50
ε_{r2} (–) (relative permittivity)	81	81	71	20	10
σ_2 (S/m) (conductivity)	0	0	0	0	0

where p_m is the modulated dipole moment, p_{OSCIL} is the oscillatory component of the dipole moment and mv is basically distance along the microtubule. Modulation function is specific for each mode, minimal mode number is zero, maximal mode number (max) depends on the number of tubulin heterodimers, i.e. length of microtubule. The mode zero represents oscillations of all dipoles in phase and the max mode represents oscillations of neighboring dipoles in antiphase.

For the illustration, modulation function of the 1st protofilament is depicted in Fig. 7 for the mode 3. Modulation functions of other protofilaments (2nd–13th) are axially shifted, according to the position of protofilaments in the real microtubule A lattice. Each circle in Fig. 7 represents the value of dipole moment of one heterodimer. Modulation function represents effect of a vibrational longitudinal wave on dipole moments of individual tubulin heterodimers. This wave can be described as the wave which has the same phase in the cutting plane orthogonal to the axis of the microtubule (Fig. 8—mode 3). Integer values of mode numbers correspond to boundary conditions of rigidly bound ends of microtubule. It is important to note that in our models of microtubule network, phase difference between oscillations of individual microtubules is zero, i.e. microtubules oscillate in phase. The distribution of electric field around microtubule excited by vibration modes min (mode 0) and max (mode 50, in this case) can be seen in Fig. 9. The intensity of

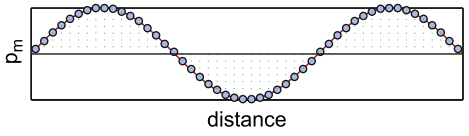


Fig. 7. The modulation function of the 1st protofilament (mode 3).

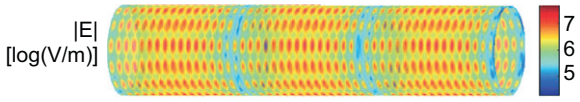


Fig. 8. The intensity of electric field in logarithmic scale on the coaxial surface 1 nm above the microtubule wall (mode 3).

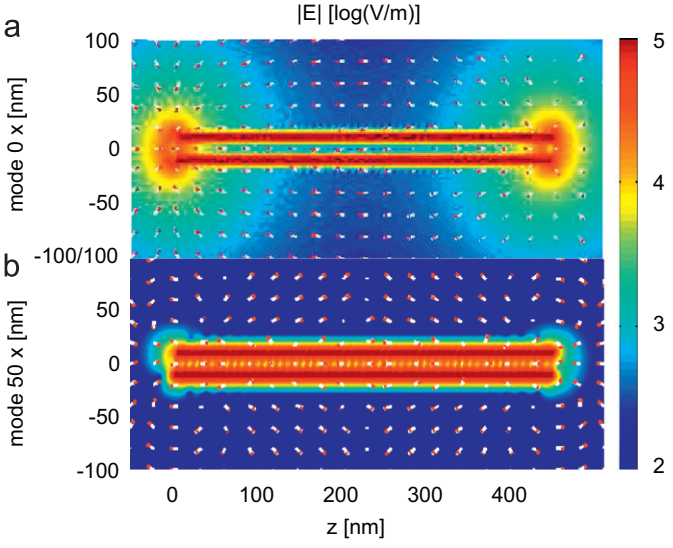


Fig. 9. The intensity of electric field in logarithmic scale in section through axis of the microtubule, which is excited by (a) mode 0 (min mode) and by (b) mode 50 (max mode).

Table 2
Total radiated power from the whole cellular microtubule network for different frequencies of the microtubule oscillations, lossless medium. The radiated power is the same both from symmetric and asymmetric model.

f (Hz)	1 k	1 M	10 M	100 M	1 G	10 G	42 G	100 G
P [log(W)]	−52.22	−40.22	−36.22	−32.22	−28.22	−24.25	−22.03	−20.68

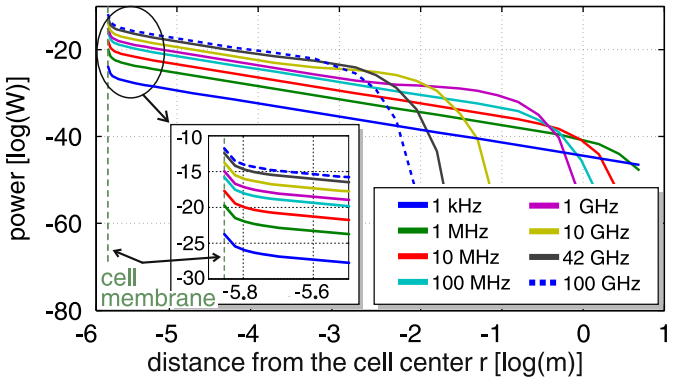


Fig. 10. Power calculated from the cell membrane to the distance of 1 m for eight frequencies (asymmetric model, mode 0 and lossy medium).

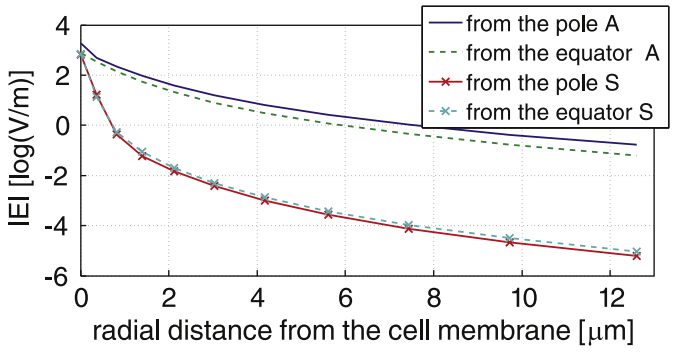


Fig. 11. Radial dependence of the electric intensity from the cell membrane in the direction from the equator (dashed lines) and from the pole (full lines) up to 12.6 μm. A and S stands for the asymmetric and the symmetric model, respectively (mode 0, f=100 GHz, lossy medium).

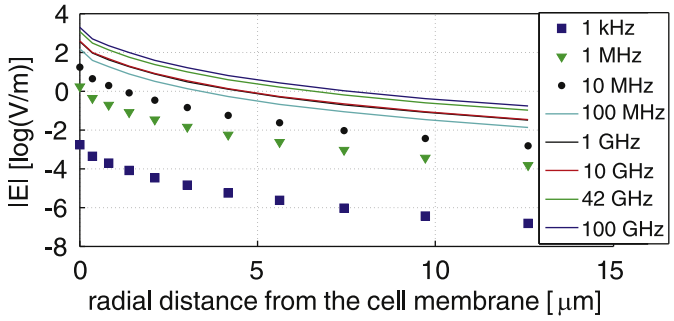


Fig. 12. Radial dependence of the electric intensity from the pole of the cell membrane—comparison of frequencies which are in the legend of the figure in Hz (asymmetric model, mode 0 and lossy medium).

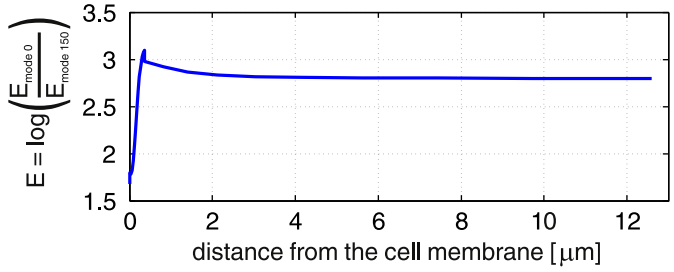


Fig. 13. Logarithm of the ratio of the electric intensity generated by mode 0 and that generated by mode 150 in dependence on radial distance from the pole of the cell membrane ($\log_{10}(E_{mode0}(r)/E_{mode150}(r))$). Electric intensity generated by mode 0 has higher values (asymmetric model, f=100 GHz and lossy medium).

electric field around microtubule generated by mode 50 is smaller by several orders of magnitude compared to electric field intensity generated by mode 0.

5. Results

At first, selected results of calculations of power of asymmetric microtubule network are presented. Eight frequencies (Table 2) and mode 0 were used for excitation of microtubules. The mode 0 is the most effective for generation of electric oscillations. Lossy and lossless medium was considered. The calculated results show that the values of radiated power from microtubule network generated by oscillations of mode min and of mode max are negligibly different (see Figs. 1–4 in supplementary material) and the values of power radiated from asymmetric and symmetric model are the same (see Figs. 5 and 6 in supplementary material). Therefore, from the calculations of radiated power results from asymmetric model only are shown. Poynting vector computed from near-field components ($E\sim 1/(\mathrm{j}kr)^3$ and $H\sim 1/(\mathrm{j}kr)^2$) has zero value in lossless medium. In contrast, the Poynting vector calculated from far field components ($E\sim 1/(\mathrm{j}kr)$ and $H\sim 1/(\mathrm{j}kr)$) is not zero. The values of power radiated from asymmetrical model in lossless medium for all eight frequencies are in Table 2.

The phase shift between near field components of intensity of electric and magnetic field is not $\pi/2$ but $\pi/2+2\phi_k$ in lossy medium (ϕ_k is a phase of propagation constant k of electromagnetic field in lossy medium, in lossless medium $\phi_k=0$). Consequently, the values of Poynting vector calculated from components of near field are not zero and are higher than Poynting vector calculated from other components in lossy medium. On the one hand the values of power near the membrane in lossy medium are higher than in lossless medium but on the other hand the values of power in lossy medium decrease steeply with distance from cell membrane. Fig. 10 shows the dependence of power generated by asymmetric microtubule network in lossy medium for all eight frequencies on radial distance. The value of power is the highest in the proximity of the cell membrane and decreases fast with growing distance.

Further results are from the calculations of intensity of electric field depending on radial distance from the pole or equator of cell (Fig. 6) for both models (Fig. 11). Fig. 12 depicts intensity of electric field depending on the distance from pole of the cell membrane for all eight frequencies. The difference between the electric intensity ΔE generated by mode 0 and that by mode 150 (maximal mode for the 1.2 μm long microtubule) in dependence of radial distance from the pole of asymmetric model in lossy medium and for frequency 100 GHz is shown in Fig. 13. The intensity of electric field on the border (at the cell membrane) of asymmetric model of the microtubule network is depicted in Fig. 14.

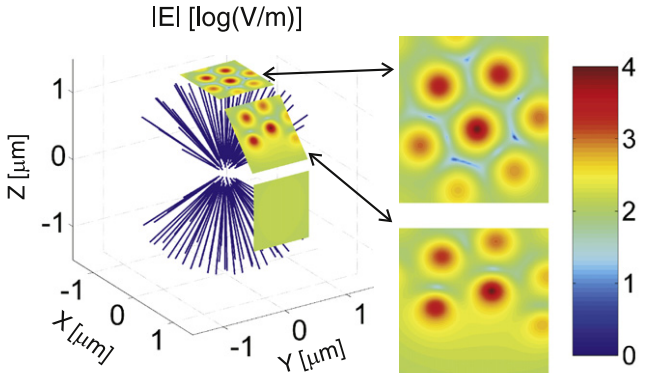


Fig. 14. The electric intensity on the border (at the cell membrane) of asymmetric model of the microtubule (mode 0, f=42 GHz, lossy medium).

6. Discussion

6.1. Approximations and assumptions on the level of the single microtubule

On the level of the single microtubule approximations and assumptions used include:

- integer mode numbers used;
- magnitude of oscillating dipole moment;
- shift of protofilaments in microtubule;
- microtubule protofilament approximated by chain of rigid particles, usage of axial longitudinal vibration modes, optical branch;
- coherent or at least quasi-coherent oscillations of individual dipoles, which require low damping of microtubule vibrations.

All of these points were discussed in the previous works of current authors (Cifra, 2009; Cifra et al., 2010d) where electric field generated by vibrations of single microtubule was already analyzed, so they are touched only briefly here.

Integer values of vibration mode number is related to boundary conditions of rigidly bound ends of microtubule. In real physiological conditions all microtubules grow from centrosome or other microtubule organizing center and can be considered to be bound rigidly (or quasi-rigidly) on the centrosome connected end (minus end). However, not all microtubules are capped and bound on its other end, the plus end. Substantial number of microtubules (exact fraction depends on the cell state and the phase of the cell cycle) undergoes dynamic instability and perpetual growth and shrinkage (Alberts et al., 2008). Vibrations of microtubules with one free end could assume infinite number of noninteger mode numbers.

Value of oscillating dipole moment used in calculations presented here represents the lower boundary of the possible values. This means that in real conditions the oscillating dipole moment can be also higher and consequently the generated electric field intensity may be higher, by approximately one order of magnitude. Axial shift of protofilaments in microtubule which was used in the model presented here corresponds to the real arrangement of protofilaments in microtubule lattice and is called lattice A, as already mentioned in Section 4. Another arrangement of protofilaments also often found in microtubules in vivo is lattice B (Tuszyński et al., 2005).

Vibrations of microtubule protofilament were approximated by vibrations of chains of rigid two-type particles, optical branch. A similar model of microtubule vibrations was used by Pokorný et al. (1997). On the level of the whole microtubule, this corresponds to axial longitudinal vibration modes of microtubules, such as treated by Wang et al. (2006), but is a special case in which neighboring tubulin particles oscillate against each other (optical branch). Vibrations of single microtubules were treated based on tubulin atomic coordinates obtained from crystallography (Deriu et al., 2010) but this approach is not computationally feasible for the whole cellular microtubule network. Therefore the approximation of tubulin as single rigid particles is considered reasonable for the current purpose.

Calculations presented here assume that there are coherent or at least quasi-coherent oscillations of individual dipoles (tubulin heterodimer). Coherent excitation can be provided by external coherent electromagnetic radiation or can be provided endogenously if system of oscillators fulfills conditions such as described by Fröhlich (1968a,b, 1980). Microtubules fulfill necessary conditions of the Fröhlich system (Cifra, 2009). Recently, Reimers et al. (2009) and McKemmish et al. (2009) performed computational studies of Fröhlich system based on using Wu–Austin Hamiltonian. They concluded that condensation of energy in certain modes strong enough to provide coherent excitations (one of the main features of Fröhlich system) is not feasible in biological systems. It is not necessary to go into details here but it has been pointed out (Cifra et al., 2010a,b) that the studies of Reimers and McKemmish treat incomplete Fröhlich system (nonlinear temperature dependence of coupling coefficients is missing) and contains several further flaws. Also another group of authors (Salari et al., 2011) noticed several errors in Reimers' study. Thus, conclusion of Reimers et al. (2009) and McKemmish et al. (2009) that the "…coherent Fröhlich condensates are not biologically feasible,…" cannot be fully accepted and definitely cannot be used for overgeneralization.

6.2. Damping of microtubule vibrations

Regardless of the mechanism for selective excitation of certain microtubule mode, it is necessary that the modes to be excited have low damping so the energy may be stored quasi-coherently in them. This requires that the energy supplied to microtubules is not dissipated rapidly to surrounding medium. Physically the problem is related to the damping of microtubule vibrations. If the microtubule vibrations are treated classically like for a cylinder immersed into bulk water, the result will be that the vibrations will be overdamped (Foster and Baish, 2000), i.e. $Q<1$ (Q, quality factor of oscillations). This may not be the case if one considers ions on the microtubule surface behaving as a slip layer (Pokorný, 2005), especially for longitudinal vibrations where negligible or no water at all will be displaced as for example in the case of standing waves with a zero vibration amplitude at the ends of microtubule. The quality factor (and the lifetime) of the biomolecule vibrations depends also on the organization of the water around the biomolecule surface: the higher the ability of the surface to attract water molecules (i.e. the higher the hydrophilicity of the surface), the higher is the Q (and lifetime) of the vibrations (Liu et al., 2009a,b). The physical mechanism is such that the water due to the electric polarity of its molecules is organized by the electric field of the surface charge of the hydrophilic biomolecule and the water undergoes visco-elastic transition (Van Zandt, 1986, 1987). There is extensive experimental evidence that the water is organized at the hydrophilic surfaces. Several layers of organized water molecules above the biomolecule interface can be detected and visualized by atomic force microscopy (Fukuma, 2010; Kimura et al., 2010). However, ordering of the water is not a matter of only a few molecular layers but can extend to macroscopic distances from strongly hydrophilic interfaces, e.g. few hundreds of micrometers as in the case of exclusion zone found by Zheng and Pollack (2003) and Zheng et al. (2006). These zones carry their name "exclusion zones" after the process they are

visualized with; the zones exclude micrometer sized particles (e.g. latex particles) in such a manner that two distinct water phases (zones) are visible at the hydrophilic interface observed under the microscope. The zone of water adjacent to the surface contains no particles (they are excluded to the outer zone), while beyond rather sharp boundary, particles are present in the second, outer water zone. It was experimentally proved that the organized water in the exclusion zone has different physical properties compared to bulk water including higher viscosity (Pollack et al., 2006), lowered thermal motion of molecules (Zheng et al., 2006), further it exhibits separation of charge, different pH (Chai et al., 2009), different spectroscopic properties (Chai et al., 2008), solvent exclusion (Zheng and Pollack, 2003; Zheng et al., 2006) and that infrared radiation promotes formation of the exclusion zones (Chai et al., 2009), etc. (Pollack et al., 2006, 2009).

Direct evidence of damping can be obtained from spectroscopy. While some spectroscopic and theoretical studies suggest that collective vibrations of proteins are overdamped by the water (Hayward et al., 1993) which is a major constituent of the cytosol, there are indications (Romanovsky et al., 2003) that the broadening of the spectral lines (a physical signature of a damping) may not be solely due to the damping but also due to inhomogeneous broadening of the spectral line—slight difference in the mode frequency due to conformational differences in the protein molecules in the ensemble under study. Actually, nonlinear spectroscopy already brought experimental evidence that lifetime (similar to quality factor Q of the oscillating system—inversely proportional to damping) of certain protein modes can be rather large, over 1000 (Xie et al., 2001). Currently, published data from direct spectroscopic studies on microtubules in MHz–GHz region are very limited. Hameroff et al. (1986) reported 8 GHz acoustic mode of microtubules with Brillouin spectroscopy, from the sole figure they provided the half width of the peak (Δf) is about 2 GHz, giving Q factor ($f/\Delta f$) about 4. Pizzi et al. (2011) measured very weak microwave absorption (0.5 dB) of in vitro microtubules with mean length of 2 μm at 1510 MHz which probably corresponds to some bending modes of microtubules which are overdamped (Samarbakhsh, 2010). Regarding these two past and any future experiments, it needs to be noted that inhomogeneous broadening contributes to broadening of the peak, thus leads to underestimation of the real Q factor. If the spectral resolution of the spectroscopy technique used is low, multiple spectral peaks will be merged into one broad peak, additionally clouding the real Q factor of oscillations. Further, longitudinal axial modes (which are most electromagnetically active in comparison with twisting or bending modes because the "stretching" of the tubulin dipole moment is greatest for longitudinal axial wave on microtubule) which conserve microtubule length will be damped much more weakly since they do not cause any displacement of the surrounding water. It is also important to realize that microtubules are naturally present in a cellular environment where the surrounding water is strongly organized due to numerous interfaces (Pollack, 2001) and by strong static electric field of mitochondria (Tyner et al., 2007). It can be expected that the in vivo damping of microtubule elastic vibrations will be lower than that measured on extracted microtubules. This can be reasonable if the amplitude of oscillations is small and comparable to size of damping units (water molecules or water clusters). In such case, classical hydrodynamic treatment of the damping (Stokes' formula) fails (Mitrofanov et al., 2006) and it underestimates the Q factor of protein oscillations especially in the THz region.

6.3. Related works on microtubule and protein vibrations (low-frequency phonons)

It may be of interest for readers to discuss several related works of Sinkala (2006) and Chou et al. (1994) and their relation to the topic of the current paper. Sinkala analyzed possibility of soliton/exciton transport in proteins which would enable non-dissipative transport of energy and related his model to the model of Resonant Recognition Model of Cosic (1994). The main connection with the current work is that solitons treated in Sinkala's paper are having low-frequency phonon (vibrational) component. In the current work, low frequency (low compared to higher frequencies of the protein vibrations) collective vibrations of the whole microtubules are the basis for the calculation of the distribution of the electric field around them. However, vibrations considered in the current paper are not of the soliton type but of simple standing harmonic wave of longitudinal axial type, optical branch, as described in our earlier paper focused on the field calculation around single microtubules (Cifra et al., 2010d). Chou et al. (1994) has focused on the soliton-like solution of the kink waves generated by the GTP hydrolysis and the possible role of these waves in the regulation of the microtubule polymerization dynamics. In the current paper, we focus on the electric field characteristic of the whole microtubule network. Regarding Davydov's solitons in proteins (namely the α-helix) and its relation to the generation of electromagnetic field we can refer reader to the works of Brizhik (Brizhik and Eremko, 2001, 2003; Brizhik, 2003), where emission of electromagnetic waves due to acceleration of the soliton involving charge transfer has been studied. The connecting work between microtubule soliton propagation and electric field generation seems to be in work of Satarić and Tuszyński. They carried out analysis of propagation of soliton type (kink) of tubulin dipole moment tilt on protofilament, which can have effect on microtubule polymerization kinetics (Satarić et al., 1992), energy transfer along microtubules (Satarić et al., 1993; Trpisová and Tuszyński, 1997), provide a possible elucidation of the unidirectional transport of cargo via motor proteins (Sataric and Tuszyński, 2005; Sataric et al., 2008). To summarize this paragraph regarding microtubules, soliton propagation and intrinsic microtubule electric field, it can be said that another approach to the problem treated in this paper could be based on calculation of electric field around microtubules generated by propagation of solitons on microtubules involving phonon–charge or phonon–dipole interaction.

6.4. Approximations and assumptions on the level of the whole cellular microtubule network

Regarding the model of the whole cellular microtubule network there are following approximations in the models in the study presented here:

- geometry of the models,
- in phase and single frequency oscillations of individual microtubules,
- size of the cell.

Geometry of the symmetric model was chosen to correspond to geometry of nondividing cell (interphase). Asymmetric model cannot be attributed to specific phase of the cell cycle, although it resembles the position of astral microtubules during the cell division. Asymmetric model was constructed in order to study influence of simple asymmetry of cytoskeleton distribution on radiation and electric field characteristic. Current work of the present authors involves modeling of complete mitotic spindle—microtubule formation during the cell division. It should be also noted that the microtubule organizing center (centrosome in many eukaryotic cells) is not always located in the center of the cell, so the microtubules do not grow exactly radially from the cell center.

In the model used in the study presented here the mutual phase difference between oscillations of individual microtubules is zero, i.e. microtubules oscillate in phase. This situation is probably very natural. Oscillations of individual microtubules can be coupled mechanically through the centrosome (or other microtubule organizing center) from which microtubules grow and coupling can be also established via microtubule electrodynamic field. From the time of Huygens it is known and nowadays very well established that coupled oscillators tend to synchronize each other (Bennett et al., 2002) in frequency (see Maffezzoni, 2010 for illustration) under certain conditions. In principle, even if the microtubules are of different length, they can support oscillations of the same frequencies (same modes). The condition of in phase oscillations of microtubules also corresponds to the requirement of minimal energy of the system. The radiation rate is lowest for such configuration since geometrical symmetry together with in phase oscillations causes effective canceling of radiative component of generated electromagnetic field. In the case when the minimum energy state is perturbed, models using random or quasi-random phase distribution of microtubules on the one hand or models using opposite phases of microtubule on opposite hemispheres on the other hand could be used.

Size of the cell (diameter 2.8 μm) used in models presented here corresponds to a rather small cell since typical diameter e.g. of standard eukaryotic model cell, yeast *Saccharomyces Cerevisiae* is 5−10 μm. Nevertheless, the total amount of microtubules used in current model corresponds to amounts present in larger cells. Work in progress includes parametric analysis of influence of number of microtubules and cell sizes on radiated power and electric field intensity at the cell membrane.

6.5. Discussion of results

Intensity of electric field and magnitude of the radiated power are comparable with the results obtained from the calculations using membrane proteins as the sources of the electric oscillations (Pokorný and Wu, 1998). Models presented here give good quantitative estimates of power and intensity of the cellular microtubule network unperturbed and unloaded by the detection electrodes. However, few other biophysical aspects influencing the technical requirements for measurement system (Kučera et al., 2010) could not be covered in current models. Electrodynamic activity probably arises from coupled oscillatory system of polar cellular structures, i.e. cytoskeleton coupled to membrane. Vibrations excited at various points of the membrane (e.g. where the cytoskeleton binds to the cell membrane) would create very complex interference pattern of multiple standing waves on the membrane. In such general case, spatial distribution of electric field intensity associated with the vibrations of the membrane will resemble high order spherical harmonics, having closely spaced regions of opposite orientation of the electric field vector. In order to resolve the spatial minima and maxima, detector electrode needs to have tip with radius of few hundreds of nanometers, ideally units of nanometers. Another aspect is related to the "softness" of the source. Providing the Q factor of oscillating system is high, energy accumulates in the system. Once the system is loaded by the detector and the energy is drained, the effective power supplied to the detector drops to the value of power delivered by the metabolism.

Models presented here do not take into account the effect of the cell membrane. It should be noted that the cell membrane behaves due to its capacitive character as a high pass filter. Therefore electric oscillations up to few MHz (or up to few hundreds of kHz only, depending on the cell type and effective capacitance of its membrane) (Asami and Yonezawa, 1996; Wang et al., 1993) which originate inside the cell cannot pass through the membrane. However, if there are mechanical vibrations present in cytoskeleton, they can be transferred into cell membrane through the cytoskeleton-membrane protein junctions. Consequently, electric oscillations can be generated by vibrations of the polar cell membrane.

7. Conclusion

Electromagnetic radiation and electric field of the whole cellular network consisting of 100 microtubules have been calculated for microtubule oscillations in the frequency region from 1 kHz to 100 GHz. Two basic models have been used for microtubule distribution, symmetric and asymmetric model. Microtubules are uniformly distributed in the symmetric model and they are distributed toward the poles of the cell in the asymmetric model. Total radiated power of the single cell for the lossless medium from the symmetric model is the same as from asymmetric model, being highest (10^{-20} W) for the highest frequency (100 GHz) calculated and lowest (10^{-52} W) for the lowest frequency (1 kHz) calculated. Electric field intensity of the symmetric model decreases steeper with the distance from the cell membrane than that of the asymmetric model, the difference is 4 orders of magnitude at the distance of 10 μm.

From current results, there are serious implications for the measurement system which is aimed to detect cellular electrodynamic activity. It is clear that macroscopic detection of the cellular far field radiation at room temperature with classical antennas is very doubtful. Cellular electrodynamic activity in radiofrequency region will be detectable under most conditions only within 10 μm from the cell membrane, conditions are more favorable when the symmetry (both phase and geometrical symmetry) of the microtubule network is perturbed. Further requirements for detectors, which cannot be quantitatively evaluated from the current models but have been enumerated and reasoned by Kučera et al. (2010), include minimal draining of the energy from biological nanosource (oscillating microtubule) and spatial resolution of hundreds to tens of nanometers. Development of sensors with these parameters is necessary to elucidate the biological role of the cellular electrodynamic activity.

Acknowledgments

The research presented in this paper was partly supported by the Grant nos. P102/10/P454, GD102/08/H008 and P102/11/0649 of the Czech Science Foundation GA CR, and by the Grant no. SGS10/179/OHK3/2T/13 of the Grant Agency of the Czech Technical University in Prague.

Appendix A. Supplementary data

Supplementary data associated with this article can be found in the online version at doi:10.1016/j.jtbi.2011.07.007.

References

Alberts, B., Johnson, A., Lewis, J., Raff, M., Roberts, K., Walter, P., 2008. Molecular Biology of the Cell, fifth ed. Garland.

Asami, K., Yonezawa, T., 1996. Dielectric behavior of wild-type yeast and vacuole-deficient mutant over a frequency range of 10 kHz to 10 GHz. Biophysical Journal 71 (4), 2192–2200. URL 〈http://www.sciencedirect.com/science/article/B94RW-4V8X9KV-1T/2/e7bf9e4fe3509087f10582c611c6ec1b〉.

Bennett, M., Schatz, M., Rockwood, H., Wiesenfeld, K., 2002. Huygens's clocks. Proceedings of the Royal Society A: Mathematical, Physical and Engineering Sciences 458 (2019), 563–579.

Betskii, O.B., Golant, M.B., Devyatkov, N.D., 1988. Millimeter waves in biology, in Russian, Millimetrovye volny v biologii. In: Fizika. Znanie, Moskva, No. 6.

Brizhik, L.S., 2003. Dynamical properties of Davydov solitons. Ukrainian Journal of Physics 48 (7), 611–622.
Brizhik, L.S., Eremko, A.A., 2001. Soliton induced electromagnetic radiation and selfregulation of metabolic processes. Physics of the Alive 12 (1), 5–11.
Brizhik, L.S., Eremko, A.A., 2003. Nonlinear model of the origin of endogenous alternating electromagnetic fields and selfregulation of metabolic processes in biosystems. Electromagnetic Biology and Medicine 22 (1), 31–39.
Bulatov, V., 1996. Distributing points on the sphere by electrostatic repulsion. 〈http://www.math.niu.edu/~rusin/known-math/96/repulsion〉.
Chai, B., Yoo, H., Pollack, G., 2009. Effect of radiant energy on near-surface water. The Journal of Physical Chemistry B 113, 13953–13958.
Chai, B., Zheng, J., Zhao, Q., Pollack, G., 2008. Spectroscopic studies of solutes in aqueous solution. Journal of Physical Chemistry A 112 (11), 2242–2247.
Chou, J.J., Li, S., Klee, C.B., Bax, A., 2001. Solution structure of Ca2+-calmodulin reveals flexible hand-like properties of its domains. Nature Structural & Molecular Biology 8 (11), 990–997.
Chou, K.C., 1984a. The biological functions of low-frequency vibrations (phonons): 4. Resonance effects and allosteric transition. Biophysical Chemistry 20 (1–2), 61–71.
Chou, K.C., 1984b. Biological functions of low-frequency vibrations (phonons). III. Helical structures and microenvironment. Biophysical Journal 45 (5), 881–889.
Chou, K.C., 1987. The biological functions of low-frequency phonons: 6. A possible dynamic mechanism of allosteric transition in antibody molecules. Biopolymers 26 (2), 285–295.
Chou, K.C., 1988. Low-frequency collective motion in biomacromolecules and its biological functions. Biophysical Chemistry 30 (1), 3–48.
Chou, K.C., 1989. Low-frequency resonance and cooperativity of hemoglobin. Trends in Biochemical Sciences 14 (6), 212.
Chou, K.C., Mao, B., 1988. Collective motion in DNA and its role in drug intercalation. Biopolymers 27 (11), 1795–1815.
Chou, K.C., Zhang, C.T., Maggiora, G.M., 1994. Solitary wave dynamics as a mechanism for explaining the internal motion during microtubule growth. Biopolymers 34 (1), 143–153.
Cifra, M., 2009. Study of Electromagnetic Oscillations of Yeast Cells in kHz and GHz Region. Ph.D. Thesis, Czech Technical University in Prague.
Cifra, M., Havelka, D., Kučera, O., 2010a. Biophysical role of oscillatory electric field generated by undamped microtubule vibrations. In: 6th International Workshop on Biological Effects of Electromagnetic Fields. Bogazici University, Istanbul.
Cifra, M., Havelka, D., Kučera, O., 2010b. Electric oscillations generated by collective vibration modes of microtubule. In: Kinnunen, M., Myllylä, R. (Eds.), Laser Applications in Life Sciences. Proceedings of SPIE, vol. 7376, p. 73760N.
Cifra, M., Havelka, D., Kučera, O., Pokorný, J., 2010c. Electric field generated by higher vibration modes of microtubule. In: 15th Conference on Microwave Techniques—COMITE 2010.
Cifra, M., Pokorný, J., Havelka, D., Kučera, O., 2010d. Electric field generated by axial longitudinal vibration modes of microtubule. BioSystems 100 (2), 122–131.
Cosic, I., 1994. Macromolecular bioactivity: Is it resonant interaction between macromolecules?—theory and applications. IEEE Transactions on Biomedical Engineering 41 (12), 1101–1114.
Deriu, M.A., Soncini, M., Orsi, M., Patel, M., Essex, J.W., Montevecchi, F.M., Redaelli, A., 2010. Anisotropic elastic network modeling of entire microtubules. Biophysical Journal 99 (7), 2190–2199. URL 〈http://www.sciencedirect.com/science/article/B94RW-515K8MN-V/2/b04f67bbda5123dade8927db98c5cb93〉.
Devyatkov, N.D., Golant, M.B., Betskii, O.B. (Eds.), 1991. Millimeter waves and their role in life processes, in Russian Millimetrovye volny i ikh rol v processakh zhiznedeyatelnosti. Moskva, Radio i svyazi.
Foster, K.R., Baish, J.W., 2000. Viscous damping of vibrations in microtubules. Journal of Biological Physics 26 (4), 255–260.
Fröhlich, H., 1968a. Bose condensation of strongly excited longitudinal electric modes. Physical Letters A 26, 402–403.
Fröhlich, H., 1968b. Long-range coherence and energy storage in biological systems. International Journal of Quantum Chemistry 2, 641–649.
Fröhlich, H., 1969. Quantum mechanical concepts in biology. In: Marois, M. (Ed.), Proceedings of First International Conference on Theoretical Physics and Biology 1967, pp. 13–22.
Fröhlich, H., 1972. Selective long range dispersion forces between large systems. Physics Letters A 39 (2), 153–154. URL 〈http://www.sciencedirect.com/science/article/B6TVM-46TY34W-18T/2/a9809a742a843a5ac0f1380c5b616209〉.
Fröhlich, H., 1975. The extraordinary dielectric properties of biological materials and the action of enzymes. Proceedings of the National Academy of Sciences of the United States of America 72 (11), 4211–4215. URL 〈http://www.pnas.org/content/72/11/4211.abstract〉.
Fröhlich, H., 1978. Coherent electric vibrations in biological systems and the cancer problem. IEEE Transactions on Microwave Theory and Techniques 26 (8), 613–618.
Fröhlich, H., 1980. The biological effects of microwaves and related questions. Advances in Electronics and Electron Physics 53, 85–152.
Fukuma, T., 2010. Water distribution at solid/liquid interfaces visualized by frequency modulation atomic force microscopy. Science and Technology of Advanced Materials 11 (3), 033003. URL 〈http://stacks.iop.org/1468-6996/11/i=3/a=033003〉.
Gordon, G., 2007. Designed electromagnetic pulsed therapy: clinical applications. Journal of Cellular Physiology 212 (3), 579–582.
Gordon, G., 2008. Extrinsic electromagnetic fields, low frequency (phonon) vibrations, and control of cell function: a non-linear resonance system. Journal of Biomedical Science and Engineering 1, 152–156.
Hameroff, S., Lindsay, S., Bruchmann, T., Scott, A., 1986. Acoustic modes of microtubules. Biophysical Journal 49(2 Pt 2), 58a, thirtieth Annual Meeting 9–13 February 1986, Brooks Hall/Convention Center, San Francisco, CA, Monday, February 10, 1986, 1:30 - 5:00 p.m., Polk Hall, Part 1.
Havelka, D., 2010. Electromagnetic field of microtubule network of the cell, in czech Elektromagnetické pole mikrotubulárního systému buňky. Master's Thesis, Czech Technical University in Prague.
Hayward, S., Kitao, A., Hirata, F., 1993. Effect of solvent on collective motions in globular protein. Journal of Molecular Biology 234 (4), 1207–1217.
Hölzel, R., 2001. Electric activity of non-excitable biological cells at radiofrequencies. Electro- and Magnetobiology 20 (1), 1–13.
Hölzel, R., Lamprecht, I., 1994. Electromagnetic fields around biological cells. Neural Network World 3, 327–337.
Jelínek, F., Cifra, M., Pokorný, J., Hašek, J., Vaniš, J., Šimša, J., Frýdlová, I., 2009. Measurement of electrical oscillations and mechanical vibrations of yeast cells membrane around 1 kHz. Electromagnetic Biology and Medicine 28 (2), 223–232.
Jelínek, F., Pokorný, J., Vaniš, J., Hašek, J., Šimša, J., 2008. Measurement of electrical and mechanical oscillations of yeast cells membrane in acoustic frequency range. In: 14th Conference on Microwave Techniques, 2008. COMITE 2008, April, pp. 1–4.
Jelínek, F., Šaroch, J., Kučera, O., Hašek, J., Pokorný, J., Jaffrezic-Renault, N., Ponsonnet, L., 2007. Measurement of electromagnetic activity of yeast cells at 42 GHz. Radioengineering 16 (1), 36–39.
Kharlanov, A.V., 2006. Acoustoelectric Vibrations of Cell, in Russian Akustoelektricheskie kolebaniya kletki. Ph.D. Thesis, Volograd State Technical University.
Kimura, K., Ido, S., Oyabu, N., Kobayashi, K., Hirata, Y., Imai, T., Yamada, H., 2010. Visualizing water molecule distribution by atomic force microscopy. The Journal of Chemical Physics 132, 194705.
Kittel, C., 1976. Introduction to Solid State Physics. John Wiley & Sons.
Kučera, O., Cifra, M., Pokorný, J., 2010. Technical aspects of measurement of cellular electromagnetic activity. European Biophysics Journal 39 (10), 1465–1470.
Liu, T., Chen, H., Wang, L., Wang, J., Luo, T., Chen, Y., Liu, S., Sun, C., 2009a. Microwave resonant absorption of viruses through dipolar coupling with confined acoustic vibrations. Applied Physics Letters 94, 043902.
Liu, T., Chen, H., Yeh, S., Wu, C., Wang, C., Luo, T., Chen, Y., Liu, S., Sun, C., 2009b. Effects of hydration levels on the bandwidth of microwave resonant absorption induced by confined acoustic vibrations. Applied Physics Letters 95 (17), 173702.
Madkan, A., Blank, M., Elson, E., Chou, K.C., Geddis, M.S., Goodman, R., 2009. Steps to the clinic with ELF EMF. Natural Science 1 (3), 157–165.
Maffezzoni, P., 2010. Synchronization analysis of two weakly coupled oscillators through a PPV macromodel. IEEE Transactions on Circuits and Systems I 57 (3), 654–663.
May, K.M., Hyams, J.S., 1998. The yeast cytoskeleton: the closer we look, the more we see. Fungal Genetics and Biology 24 (1–2), 110–122. URL 〈http://www.sciencedirect.com/science/article/B6WFV-45K17FP-10/2/07a53e5685075a04b75af212f3dc46df〉.
McKemmish, L.K., Reimers, J.R., McKenzie, R.H., Mark, A.E., Hush, N.S., 2009. Penrose–Hameroff orchestrated objective-reduction proposal for human consciousness is not biologically feasible. Physical Review E 80 (2), 021912-1–021912-6.
Mitrofanov, V., Romanovsky, Y., Netrebko, A., 2006. On the damping of the fluctuations of atomic groups in water environment. Fluctuation and Noise Letters 6 (2), L133–L145.
Pelling, A.E., Sehati, S., Gralla, E.B., Gimzewski, J.K., 2005. Time dependence of the frequency and amplitude of the local nanomechanical motion of yeast. Nanomedicine: Nanotechnology, Biology and Medicine 1, 178–183.
Pelling, A.E., Sehati, S., Gralla, E.B., Valentine, J.S., Gimzewski, J.K., 2004. Local nanomechanical motion of the cell wall of *Saccharomyces cerevisiae*. Science 305, 1147–1150.
Pizzi, R., Strini, G., Fiorentini, S., Pappalardo, V., Pregnolato, M., 2011. Evidences of new biophysical properties of microtubules. In: John, A. Flores (Ed.), Focus on Artificial Neural Networks. Nova Science Publisher, ch. 9, pp. 191–208.
Pohl, H.A., 1980. Oscillating fields about growing cells. International Journal of Quantum Chemistry: Quantum Biology Symposium 7, 411–431.
Pohl, H.A., 1981. Electrical oscillation and contact inhibition of reproduction in cells. Journal of Biological Physics 9 (4), 191–200.
Pohl, H.A., Braden, T., Robinson, S., Piclardi, J., Pohl, D.G., 1981. Life cycle alterations of the micro-dielectrophoretic effects of cells. Journal of Biological Physics 9, 133–154.
Pokorný, J., 1985. Biological effects of microwaves and cancer treatment. Mikrowellen Magazin 11 (3), 240–242.
Pokorný, J., 1987. Coherent excitation and electromagnetic field generated by living cells. In: Fiala, J., Pokorný, J. (Eds.), Biophysical Aspects of Cancer, pp. 102–110.
Pokorný, J., 1990. Electromagnetic field generated by living cells, in Czech, Elektromagnetické pole generované živými buòkami. Ph.D. Thesis. Faculty of Mathematics and Physics, Charles University.
Pokorný, J., 2001. Endogenous electromagnetic forces in living cells: implication for transfer of reaction components. Electro- and Magnetobiology 20 (1), 59–73.
Pokorný, J., 2005. Viscous effects on polar vibrations microtubules. In: URSI GA Delhi Proceedings.

Pokorný, J., 2006. The role of Fröhlich's coherent excitations in cancer transformation of cells. In: Herbert Frohlich FRS: A Physicist Ahead of his Time. University of Liverpool, pp. 177–207.
Pokorný, J., Fiala, J., 1994. Condensed energy and interaction energy in Fröhlich systems. Neural Network World 94 (3), 299–313.
Pokorný, J., Fiala, J., Skála, L., Jelínek, F., Šrobár, F., Trkal, V., 1996. Biohysical aspects of coherence and Fröhlich's theory, in Czech Biofyzikální aspekty koherence a Fröhlichovy teorie. Československý časopis pro fyziku 46 (3), 139–156.
Pokorný, J., Hašek, J., Jelínek, F., 2005a. Electromagnetic field in microtubules: effects on transfer of mass particles and electrons. Journal of Biological Physics 31 (3–4), 501–514.
Pokorný, J., Hašek, J., Jelínek, F., 2005b. Endogenous electric field and organization of living matter. Electromagnetic Biology and Medicine 24 (3), 185–197.
Pokorný, J., Hašek, J., Jelínek, F., Šaroch, J., Palán, B., 2001. Electromagnetic activity of yeast cells in the M phase. Electro- and Magnetobiology 20 (1), 371–396.
Pokorný, J., Hašek, J., Vaniš, J., Jelínek, F., 2008. Biophysical aspects of cancer—electromagnetic mechanism. Indian Journal of Experimental Biology 46 (May), 310–321.
Pokorný, J., Jandová, A., Kobilková, J., Heyberger, K., Hraba, T., 1983. Fröhlich electromagnetic radiation from human leukocytes: implications for leukocyte adherence inhibition test. Journal of Theoretical Biology 102 (2), 295–305.
Pokorný, J., Jelínek, F., Trkal, V., 1998. Electric field around microtubules. Bioelectrochemistry and Bioenergetics 48, 267–271.
Pokorný, J., Jelínek, F., Trkal, V., Lamprecht, I., Hölzel, R., 1997. Vibrations in microtubules. Journal of Biological Physics 23, 171–179.
Pokorný, J., Wu, T.-M., 1998. Biophysical Aspects of Coherence and Biological Order. Academia, Springer, Praha, Czech Republic, Berlin, Heidelberg, New York.
Pollack, G., 2001. Cells, Gels and the Engines of Life. Ebner Seattle, WA.
Pollack, G., Cameron, I., Wheatley, D., 2006. Water and the Cell. Springer, Dodrecht, The Netherlands.
Pollack, G., Figueroa, X., Zhao, Q., 2009. Molecules, water, and radiant energy: new clues for the origin of life. International Journal of Molecular Sciences 10 (4), 1419–1429.
Reimers, J.R., McKemmish, L.K., McKenzie, R.H., Mark, A.E., Hush, N.S., 2009. Weak, strong, and coherent regimes of Fröhlich condensation and their applications to terahertz medicine and quantum consciousness. Proceedings of the National Academy of Sciences 106 (11), 4219–4224. URL 〈http://www.pnas.org/content/106/11/4219.abstract〉.
Romanovsky, Y., Netrebko, A., Chikishev, A., 2003. Are the subglobular oscillations of protein molecules in water overdamped? Laser physics 13 (6), 827–838.
Rowlands, S., Sewchand, L., Enns, E., 1982. Further evidence for a Fröhlich interaction of erythrocytes. Physics Letters A 87 (5), 256–260.
Rowlands, S., Sewchand, L., Lovlin, R., Beck, J., Enns, E., 1981. A Fröhlich interaction of human erythrocytes. Physics Letters A 82 (8), 436–438.
Salari, V., Rahnama, M., Tuszynski, J.A., 2011. On the theoretical possibility of quantum visual information transfer to the human brain. 〈arXiv.org/quant-phys:0809.0008v4〉.
Samarbakhsh, A., 2010. Mechanical Properties of Bio- and Nano-filaments. Ph.D. Thesis. University of Alberta.
Sataric, M., Budinski-Petkovic, L., Loncarevic, I., Tuszyński, J., 2008. Modelling the role of intrinsic electric fields in microtubules as an additional control mechanism of bi-directional intracellular transport. Cell Biochemistry and Biophysics 52 (2), 113–124.
Sataric, M., Tuszyński, J., 2005. Nonlinear dynamics of microtubules: biophysical implications. Journal of Biological Physics 31 (3), 487–500.
Satarić, M., Tuszyński, J., Žakula, R., 1993. Kinklike excitations as an energy-transfer mechanism in microtubules. Physical Review E 48(1), 589.
Satarić, M., Žakula, R., Tuszyński, J., 1992. A model of the energy transfer mechanisms in microtubules involving a single soliton. Nanobiology 1 (4), 445–456.
Schnell, J.R., Chou, J.J., 2008. Structure and mechanism of the M2 proton channel of influenza A virus. Nature 451 (7178), 591–595.
Shein, A.G., Kharlanov, A.V., 2007. Dipole representation of the membrane, in Russian Dipolnoe predstavlenie membrany. Biomedtsinskie tekhnologii i radioelektronika (5), 15–19.
Sinkala, Z., 2006. Soliton/exciton transport in proteins. Journal of Theoretical Biology 241, 919–927.
Sobel, S.G., 1997. Mini review: mitosis and the spindle pole body in saccharomyces cerevisiae. The Journal of Experimental Zoology 277 (2), 120–138.
Trpisová, B., Tuszyński, J.A., 1997. Possible link between guanosine 5' triphosphate hydrolysis and solitary waves in microtubules. Physical Review E 55 (3), 3288.
Tuszyński, J., Brown, J., Crawford, E., Carpenter, E., Nip, M., Dixon, J., Sataric, M., 2005. Molecular dynamics simulations of tubulin structure and calculations of electrostatic properties of microtubules. Mathematical and Computer Modelling 41 (10), 1055–1070. URL 〈http://www.sciencedirect.com/science/article/B6V0V-4HBSKN3-2/2/696be29f0574687723502f8017c628c5〉.
Tyner, K.M., Kopelman, R., Philbert, M.A., 2007. "Nano-sized voltmeter" enables cellular-wide electric field mapping. Biophysical Journal 93, 1163–1174.
Van Zandt, L.L., 1986. Resonant microwave absorption by dissolved DNA. Physical Review Letters 57 (16), 2085–2087.
Van Zandt, L.L., 1987. Why structured water causes sharp absorption by DNA at microwave frequencies. Journal of Biomolecular Structure & Dynamics 4 (4), 569.
Vermont Photonics Technologies Corp., 2011. URL 〈http://homepages.sover.net/~bell/newfrontierpics.htm〉.
Wang, C., Ru, C., Mioduchowski, A., 2006. Vibration of microtubules as orthotropic elastic shells. Physica E: Low-dimensional Systems and Nanostructures 35 (1), 48–56. URL 〈http://www.sciencedirect.com/science/article/B6VMT-4KJTNT4-2/2/c937e65ac2d9b1c7e4f0449b66f544b0〉.
Wang, J.F., Chou, K.C., 2009. Insight into the molecular switch mechanism of human Rab5a from molecular dynamics simulations. Biochemical and Biophysical Research Communications 390 (3), 608–612.
Wang, X.B., Huang, Y., Hölzel, R., Burt, J.P.H., Pethig, R., 1993. Theoretical and experimental investigations of the interdependence of the dielectric, dielectrophoretic and electrorotational behaviour of colloidal particles. Journal of Physics D: Applied Physics 26, 312.
Winey, M., Mamay, C., O'Toole, E., Mastronarde, D., Giddings Jr, T.H., McDonald, K., McIntosh, J., 1995. Three-dimensional ultrastructural analysis of the Saccharomyces cerevisiae mitotic spindle. Journal of Cell Biology 129 (6), 1601–1615. URL 〈http://jcb.rupress.org/cgi/content/abstract/129/6/1601〉.
Xie, A., van der Meer, A., Austin, R., 2001. Excited-state lifetimes of far-infrared collective modes in proteins. Physical Review Letters 88 (1), 18102-1–18102-4.
Zheng, J., Chin, W., Khijniak, E., Khijniak Jr., E., Pollack, G.H., 2006. Surfaces and interfacial water: evidence that hydrophilic surfaces have long-range impact. Advances in Colloid and Interface Science 127 (1), 19–27.
Zheng, J., Pollack, G., 2003. Long-range forces extending from polymer-gel surfaces. Physical Review E 68 (3), 31408-1–31408-7.